

Photoinduced Multistable Phenomena in the Tunneling Current through Doped Superlattices

Ramón Aguado^{1,2} and Gloria Platero²

¹*Department of Applied Physics, Delft University of Technology, P.O. Box 5046, 2600GA, Delft, The Netherlands*

²*Departamento de Teoría de la Materia Condensada, Instituto de Ciencia de Materiales (CSIC) Cantoblanco, 28049 Madrid, Spain*
(Received 15 May 1998)

We investigate theoretically the effect of intense THz radiation on the nonlinear properties of doped semiconductor superlattices (SL's). For the first time, the fully nonlinear current through the SL with an arbitrary combination of ac and dc voltages is calculated from a microscopic self-consistent model. We focus on the formation of electric field domains and the appearance of new multistability regions caused by the interplay of the strong nonlinearity, due to the Coulomb interaction, and the new photon-assisted channels. For low dc bias voltages and for some frequencies and intensities of the ac field the system is bistable with either positive or negative electron pumping. [S0031-9007(98)07733-3]

PACS numbers: 73.40.Gk, 73.50.Fq, 73.50.Mx

Recently, the time-dependent transport properties of semiconductor nanostructures have been the subject of interest [1–3]. Among the time-dependent phenomena in these systems one might consider photon-assisted tunneling (PAT), electron pumps, turnstiles, and others; most of them necessitate an analysis beyond linear response theory in the external frequency. The nonlinear properties having their origin in Coulomb interaction have attracted a great deal of attention as well. A doped semiconductor superlattice (SL) is a paradigm of a nonlinear system where all the intrinsic properties (multistability, bifurcations to chaos, electric field domains formation, and self-sustained current oscillations) can be routinely modified by the application of an external dc voltage or by the modification of the doping [4–10]. In this Letter we deal with PAT in weakly coupled doped SL's whose transport mechanism is sequential tunneling. In this regime the intrinsic minibandwidth is typically 1 order of magnitude smaller than the scattering induced broadening (for the samples of Ref. [1] the minibandwidth is ~ 0.1 meV). In this case, miniband transport can be neglected and transport at low bias voltages is governed by sequential resonant tunneling [1,11,12].

Our self-consistent microscopic model for PAT allows, for the first time, a systematic study of the low and the high dc bias regime with special emphasis on nonlinear effects. In the high dc bias region, we discuss the new electric field domains supported by PAT channels and the formation of new multistability regions induced by the THz field. These nonlinearities in the I - V_{dc} characteristics can be externally controlled by modifying the intensity and frequency of the ac field. In the low dc bias region and in the dynamical localization (DL) regime, i.e., where the direct tunneling channel is blocked [13–

16], the system is bistable with either negative or positive current.

In order to calculate the fully nonlinear current of a doped SL with an arbitrary combination of dc and high frequency ac voltages, an extension of the self-consistent model of Ref. [17] is put forward. This microscopic model has been generalized for including the effects coming from the THz field. In the tunneling Hamiltonian scheme [3], these effects are included considering that the single particle energies in the different isolated regions of the structure (leads and wells) become time dependent before the tunneling couplings are switched on [3,11,13]: $\epsilon_{k,i}(t) = \epsilon_{k,i}^0 + eV_i(t)$. Here, $\epsilon_{k,i}^0$ represents the electronic energy for $i = L, R$ (left and right lead, respectively) and k labels the electronic state before connecting the different regions [3]. At the wells, $\epsilon_{n,i}(t) = \epsilon_{n,i}^0 + eV_i(t)$ ($\epsilon_{n,i}^0$ is the energy of the n th resonant state at the i th well). The time-dependent voltage in the i th region is $V_i(t) = V_i \cos \omega t$. This approximation is valid for driving frequencies smaller than the plasma frequency [3]. The occupation in the contacts was determined in the past by Fermi-Dirac distributions before all the perturbations were turned on. Because of the time dependence of the external field the single particle propagators acquire phase factors coming from the breakdown of time translational invariance. After establishing the time dependence, the different regions are connected by means of the tunneling Hamiltonian [3,18,19]. We obtain the transmission probability from the i th quantum well to the $(i + 1)$ th quantum well, from the emitter to the first quantum well, and from the N th quantum well (N is the number of quantum wells) to the collector. From these probabilities we calculate the time averaged sequential currents [11]. The current from the i th well to the $(i + 1)$ th well is

$$J_{i,i+1} = \frac{2e\hbar k_B T}{\pi^2 m^*} \sum_{j=1}^{n_{\max}} \sum_{m=-\infty}^{\infty} J_m^2(\alpha) \int \frac{\gamma}{(\epsilon - \epsilon_{C1}^i)^2 + \gamma^2} \frac{\gamma}{(\epsilon - \epsilon_{Cj}^{i+1} + m\hbar\omega)^2 + \gamma^2} T_{i+1}(\epsilon, \epsilon + m\hbar\omega) \times \ln \left[\frac{1 + e^{\frac{\epsilon_{\omega j} - \epsilon}{k_B T}}}{1 + e^{\frac{\epsilon_{\omega j+1} - \epsilon - m\hbar\omega_0}{k_B T}}} \right] d\epsilon. \quad (1)$$

In these expressions, J_n is the Bessel function of first kind with argument $\alpha = \frac{eFd}{\hbar\omega}$ [$Fd = V_{i+1} - V_i$ is the potential drop between the i th well and the $(i + 1)$ th well due to the time-dependent electric field of intensity F and d the period of the SL], ϵ_{Cj}^i is the j th resonant state of the i th well (n_{\max} is the number of subbands participating in the transport), and $T_i(\epsilon, \epsilon + m\hbar\omega)$ is the inelastic transmission through the i th barrier [13]. T is the temperature at the contacts [20]. The current from the emitter to the first well, $J_{0,1}$, and the one from the N th well to the collector, $J_{N,N+1}$, are also derived in our model. Scattering is treated phenomenologically by considering the spectral functions of the wells as Lorentzians (γ is the half width). Relaxation in the planes perpendicular to the transport direction is considered imposing current conservation through the whole structure. It determines the sequential current J as well as the Fermi energies ϵ_{ω_i} —which define the charge densities n_i —within each well. In the stationary regime, for a given set of $N + 1$ unknowns $\{J, \epsilon_{\omega_i}\}$ the currents have to fulfill the set of $N + 1$ rate equations [17]:

$$J_{i-1,i} = J_{i,i+1} = J, \quad i = 1, \dots, N. \quad (2)$$

In the time-dependent case a form of Ampère's law, which explicitly contains the displacement currents, can be derived [17]. The assumption of having Fermi distribution functions in the wells considers implicitly some scattering mechanism that thermalizes the electrons after each tunneling event. Our approximation that makes the numerical calculation tractable could be improved by a direct substitution of the spectral functions for those for impurity scattering or interface roughness [12]. If there were no mechanism for obtaining thermal equilibrium, the distribution functions in the wells would be nonequilibrium functions to be calculated [18]. The formation of regions inside the SL with high electron densities leads to the nonlinear behavior of the system. Because of this nonlinearity, it is crucial to perform a self-consistent calculation, for each applied bias voltage, V_{dc} . We include the Coulomb interaction in a mean field approximation by means of discrete Poisson equations relating the potential drops in wells (N unknowns), barriers ($N + 1$ unknowns), and contacts (2 unknowns). The boundary conditions at the contacts contain four equations describing the lengths of the depletion and accumulation layers as well as the charge density at the leads (4 unknowns). The other unknowns are the Fermi energies in the wells (N unknowns) and the sequential current. The final set of $3N + 8$ equations and unknowns is closed by two equations of conservation of charge and voltage (the sum of the local potential drops has to be equal to the applied voltage, V_{dc}) and by the $N + 1$ rate equations (see Ref. [17] for a detailed discussion of the self-consistent model). The current depends explicitly on the Fermi levels and potential drops (through the resonant level positions ϵ_{Cj}^i) and implicitly through the transmissions (which depend on the local electrostatic distribution). The numerical procedure (continuation method

[21]) allows one to obtain both the stable and unstable solutions as well as all the multistability regions in the I - V_{dc} curve.

The expression for the current [Eq. (1)] is formally equivalent to the well established relation between the tunneling current with and without an ac field through a barrier, known as the Tien-Gordon (TG) formula $I_{ac}(V_{dc}) = \sum_{n=-\infty}^{\infty} J_n^2(\alpha) I_{dc}(V_{dc} + n\hbar\omega)$ [22].

This relation, however, holds only for situations where the Coulomb interaction is neglected [11,12]. In our problem, the ac field modifies the charge densities (and therefore the rest of the variables which are modified in a self-consistent way). This dependence on the charges leads to the nonvalidity of the TG formula [23].

We study the I - V_{dc} characteristics of a SL consisting of ten wells of 90 Å GaAs separated by 40 Å Ga_{0.5}Al_{0.5}As barriers. The doping at the leads and at the wells are, respectively, $N_D = 2 \times 10^{18} \text{ cm}^{-3}$ and $N_D^w = 1.5 \times 10^{11} \text{ cm}^{-2}$ ($\gamma = 2 \text{ meV}$ and $T = 0 \text{ K}$). In the static case (not shown for brevity), the low dc bias voltage peak is determined by $C1^i$ - $C1^{i+1}$ sequential tunneling through the whole SL. At higher V_{dc} the current evolves along a series of branches. This behavior can be explained by the formation of a charge accumulation layer in one of the wells (domain wall) [4–6,8] that splits the SL into two regions with low and high dc electric field, respectively. Increasing V_{dc} , this charge cannot move continuously through the SL. This motion can occur only for voltages allowing resonant interwell tunneling. In this situation, the domain wall moves from the i th well to the $(i - 1)$ th well and the electrostatic configuration becomes unstable, leading to a new one in which the i th well drops in the high electric field region. For some values of the doping of the wells this instability leads to an oscillatory behavior of the domain wall, with recycling at the contacts, that does not evolve towards an stationary state. In this regime the current oscillates (self-sustained current oscillations [5,7]) with a frequency that depends on the applied dc bias voltage. Nonetheless, in this work we will concentrate on the stationary regime; in this case the electrostatic instability leads to a series of sharp discontinuities in the I - V_{dc} curve.

In Fig. 1 we study the formation of electric field domains in the presence of the THz field. Our calculation shows that the virtual PAT channels (i.e., emission and absorption) support electric field domains: in the inset we plot the calculated potential profile of the SL for $V_{dc} = 0.86 \text{ V}$ (the dashed lines represent the PAT channels). The high field domain is supported by $C1^i$ - $C2^{i+1}$ tunneling involving absorption of two photons. This effect has been observed experimentally in a different sample [1]. Increasing the intensity, multiphotonic effects show up and new multistability regions are induced (Fig. 2). The inset shows a magnification of the first branch; the circles mark the stable operating points for a fixed V_{dc} . At $V_1 = 0.16 \text{ V}$ transport in the high field domain occurs via tunneling between the

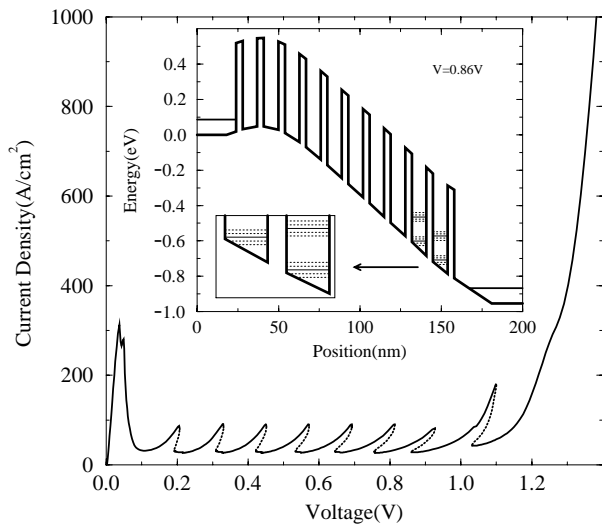


FIG. 1. $I-V_{dc}$ characteristic for the SL with ac, $F = 0.47 \times 10^6$ V/m, $\omega = 3$ THz. The continuous (dotted) lines are the stable (unstable) solutions. The inset shows the calculated potential profile at $V_{dc} = 0.86$ V (dashed lines represent PAT channels).

two-photon absorption virtual state associated with $C1^i$ and the two-photon emission virtual state associated with $C2^{i+1}$. At $V_2 = 0.19$ V the branch develops a multistable solution (five solutions coexist, three stable and two unstable). These solutions involve a different number of photons emitted in C2: one photon in the highest current stable solution (circle *a*), and two photons in the lowest current stable solution (circle *c*). This situation repeats periodically as the domain wall moves through the SL giving the sawtooth structure in the current.

As a final example of the high nonlinear response of the system to the THz field, we have studied the DL condition

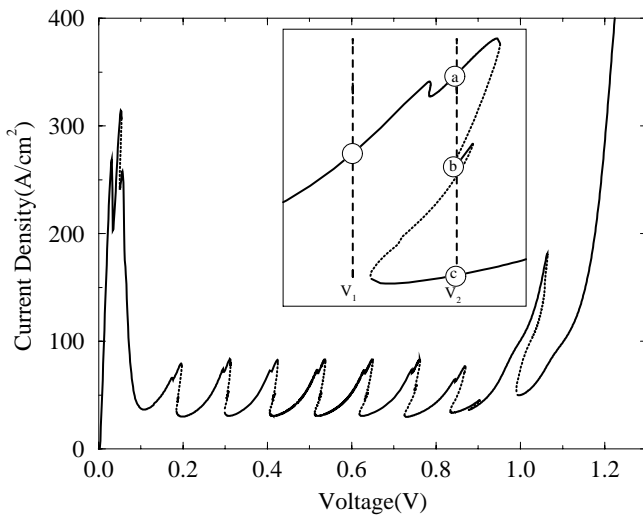


FIG. 2. $I-V_{dc}$ characteristic for the SL with ac ($F = 0.95 \times 10^6$ V/m, $\omega = 3$ THz). The inset shows a blowup of the first branch.

[13–16] (blocking of the direct tunneling channel when the parameter $\alpha = \frac{eFd}{\hbar\omega}$ is a root of the zeroth order Bessel function). In this situation transport takes place by multiphoton absorption and emission. The $I-V_{dc}$ curve at low dc bias voltages (Fig. 3) presents bistability with either positive or negative current for a fixed (positive) dc bias. Absolute negative conductance in THz irradiated SL's has been observed experimentally [1]. In order to explain these new features, we plot in Figs. 4a and 4b the electrostatic profiles at fixed bias ($V_{dc} = 0.0204$ V) for the two stable solutions (*a* and *c* in Fig. 3, respectively). This figure shows the high nonlinear potential drop through the SL even at low biases. The main difference between the electrostatic profiles at the same bias voltage comes from the energy position of the ground states and Fermi levels—not depicted for clarity—in the 8th and 9th wells (see the insets in Figs. 4a and 4b). In the case 4a, the current flows from the 8th well towards the 9th well by absorption of a photon in the 8th well (positive current). The 8th well splits the SL in two regions with different transport mechanisms. At the left side of this well, i.e., from the emitter to the 8th well, the transport is regulated by stimulated emission of photons while from the 8th well to the collector the transport is regulated by absorption. In the case 4b, we have the opposite situation: the current flows from the 9th well towards the 8th well by absorption of one photon in the 9th well (negative current). The 9th is now the boundary between two different transport mechanisms: absorption at the left of the 9th well towards the emitter and stimulated emission from the 10th well to the 9th well.

This interplay between different transport mechanisms in the SL leads to this bistable situation. We should point out, however, that a treatment of the optical response

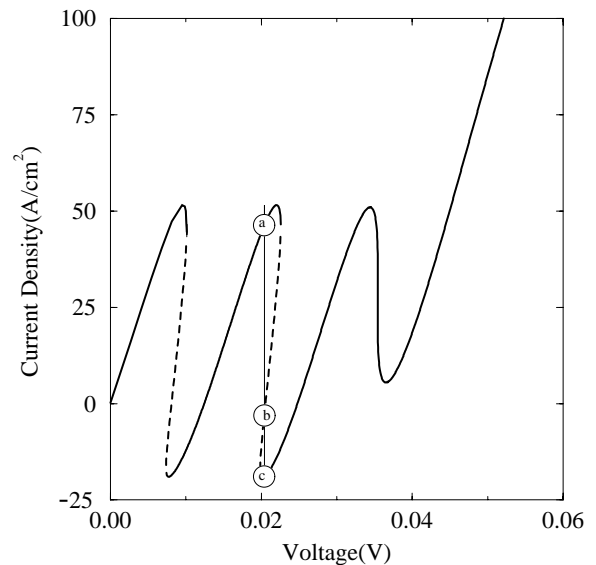


FIG. 3. $I-V_{dc}$ characteristic for the SL (sample *a*) at low bias ($F = 1.14 \times 10^6$ V/m, $\omega = 1.5$ THz).

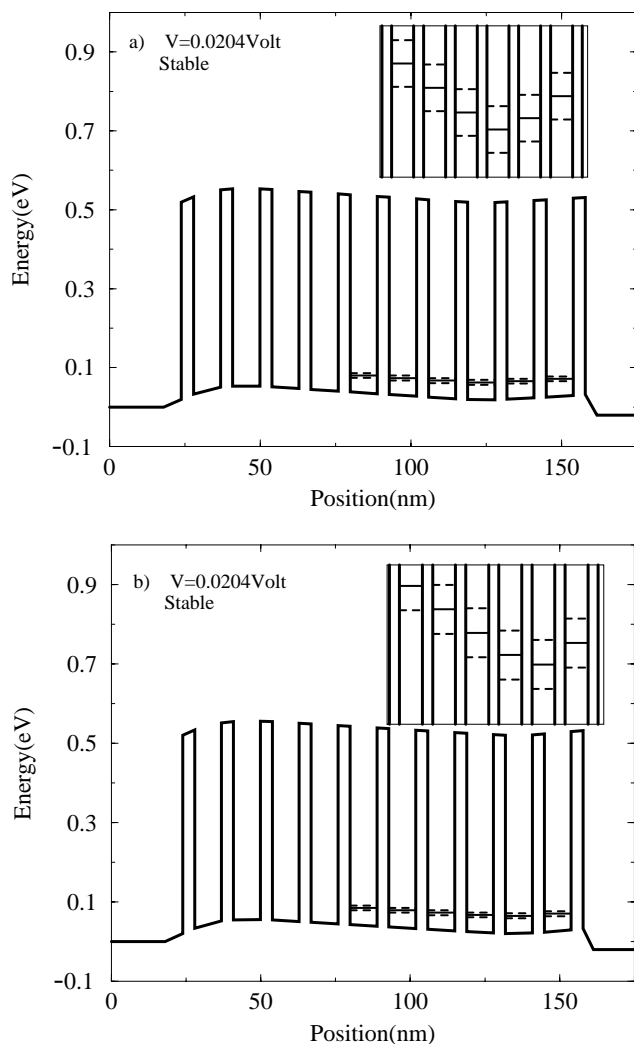


FIG. 4. (a) Electrostatic profile at $V_{dc} = 0.0204$ V, for the stable current solution (a) of Fig. 3. (b) Same as in (a) for the stable current solution (c) of Fig. 3. (Insets show a magnification of the wells 5–10.)

of the sample to a THz field would be necessary in order to obtain the fully nonlinear behavior of the system [24]. In summary, we have proposed and solved, for the first time, a microscopic self-consistent model for the sequential current through a doped SL in the presence of THz radiation. In general, and due to Coulomb interaction, the TG formula is not valid. We have shown that the electric field domains can be supported by the virtual PAT sidebands. Multiphotonic effects lead to the appearance of multistability regions in the I - V_{dc} curve. At the DL condition and low dc bias voltages, the nonlinear response of the SL to the THz field manifests as bistability in the sign of the current.

We acknowledge A. P. Jauho, K. K. Likharev, and N. S. Wingreen for their valuable comments and criticism. Also we acknowledge L. L. Bonilla and M. Moscoso for fruitful collaboration on related topics. This work has been supported by the CICYT (Spain) No. PB96-0875 and by the EU via Contract No. FMRX-CT98-0180.

- [1] B. J. Keay *et al.*, Phys. Rev. Lett. **75**, 4102 (1995); B. J. Keay *et al.*, Phys. Rev. Lett. **75**, 4098 (1995); S. Zeuner *et al.*, Phys. Rev. B **53**, 1717 (1996).
- [2] L. P. Kouwenhoven *et al.*, Phys. Rev. Lett. **73**, 3443 (1994).
- [3] Antti-Pekka Jauho, Ned S. Wingreen, and Yigal Meir, Phys. Rev. B **50**, 5528 (1994).
- [4] H. T. Grahn, R. J. Haug, W. Müller, and K. Ploog, Phys. Rev. Lett. **67**, 1618 (1991).
- [5] S. H. Kwok *et al.*, Phys. Rev. B **51**, 10171 (1995).
- [6] L. L. Bonilla *et al.*, Phys. Rev. B **50**, 8644 (1994).
- [7] J. Kastrop *et al.*, Phys. Rev. B **55**, 2476 (1997).
- [8] F. Prengel, A. Wacker, and E. Scöll, Phys. Rev. B **50**, 1705 (1994).
- [9] L. Esaki and L. L. Chang, Phys. Rev. Lett. **33**, 495 (1974).
- [10] A. Wacker, M. Moscoso, M. Kindelan, and L. L. Bonilla, Phys. Rev. B **55**, 2466 (1997), and references therein.
- [11] Gloria Platero and Ramon Aguado, Appl. Phys. Lett. **70**, 3546 (1997).
- [12] A. Wacker *et al.*, Phys. Rev. B **56**, 13268 (1997).
- [13] Ramon Aguado and Gloria Platero, Phys. Rev. B **55**, 12860 (1997).
- [14] F. Grossmann, T. Dittrich, P. Jung, and P. Hanggi, Phys. Rev. Lett. **67**, 516 (1991).
- [15] M. Holthaus, Phys. Rev. Lett. **69**, 351 (1992).
- [16] M. Wagner, Phys. Rev. B **49**, 16544 (1994).
- [17] Ramon Aguado, Gloria Platero, Miguel Moscoso, and Luis L. Bonilla, Phys. Rev. B **55**, R16053 (1997).
- [18] M. Jonson, Phys. Rev. B **39**, 5924 (1989).
- [19] R. Aguado, J. Iñarrea, and G. Platero, Phys. Rev. B **53**, 10030 (1996).
- [20] For high intensities (about 1 order of magnitude higher than those considered in this work), PAT can lead to heating effects at the contacts; see H. Drexler *et al.*, Appl. Phys. Lett. **67**, 2816 (1995).
- [21] E. J. Doedel, "AUTO: Software for Continuation and Bifurcation Problems in Ordinary Differential Equations," California Institute of Technology Applied Mathematics Report, 1986.
- [22] P. K. Tien and J. P. Gordon, Phys. Rev. **129**, 647 (1963).
- [23] Recently, the same conclusion, i.e., the nonapplicability of the Tien-Gordon theory in nonlinear ac transport, has been addressed in the context of scattering theory; Morten Holne Pedersen and Markus Büttiker, cond-mat/9803306.
- [24] Avik W. Ghosh, Alex V. Kuznetsov, and John W. Wilkins, Phys. Rev. Lett. **79**, 3494 (1997).